Sulforaphane-cysteine induces apoptosis by sustained activation of ERK1/2 and caspase 3 in human glioblastoma U373MG and U87MG cells

SAI WU[1], YAN ZHOU[1], GAOXIANG YANG[1], HUA TIAN[1], YANG GENG[1], YABIN HU[1], KAI LIN[1] and WEI WU[1,2]

[1]Department of Biochemistry and Molecular Biology, School of Basic Medical Sciences, [2]Institute of Brain Tumor, Beijing Institute for Brain Disorders, Capital Medical University, Beijing, P.R. China

Received September 12, 2016; Accepted February 22, 2017

DOI: 10.3892/or.2017.5562

Abstract. We previously demonstrated that sulforaphane (SFN) inhibited invasion via sustained activation of ERK1/2 in human glioblastoma cells. However, sulforaphane-cysteine (SFN-Cys), an analog of SFN, enriched in plasma with longer half-life, had more potentiality to induce apoptosis. Here we investigated the molecular mechanisms of SFN-Cys-induced apoptosis in human glioblastoma U373MG and U87MG cells. Cell viability assay showed that SFN-Cys inhibited cell viability in a dose-dependent manner. Cell morphology observation also showed SFN-Cys increased the phenotype of cell death in a dose-dependent manner. Furthermore, flow cytometry assay showed that SFN-Cys induced apoptosis significantly in a dose-dependent manner in both cell lines. Furthermore, western blot analysis demonstrated that SFN-Cys induced activation of ERK1/2 in a sustained manner and the activation contributed to upregulation of Bax/Bcl-2 ratio and cleaved caspase 3, and these results can be reversed by the ERK1/2 blocker PD98059. Our results showed that SFN-Cys induced cell apoptosis via sustained activation of ERK1/2 and the ERK1/2 mediated signaling pathways such as activation of caspase 3 and apoptosis-related proteins, thus indicating that SFN-Cys might be a more promising therapeutic agent versus SFN to resist glioblastoma cells, especially in Taxol-resistant cancer cells.

Introduction

Brain glioblastoma is a commonly occurred tumor with aggressive features. The therapeutic way to treat this disease is to use a surgical resection followed by a combination of radiotherapy and/or temozolomide (TMZ) chemotherapy (1). However, glioblastoma cells often generate resistance to TMZ treatment and the average survival time for patients after general treatment is ~15 months (2,3). Therefore, it is essential to find an effective agent to treat glioblastoma, especially drug-resistant glioblastoma.

Numerous studies have suggested that sulforaphane (SFN) obtained from cruciferous vegetables induced apoptosis in a variety of tumors (4-7). *In vivo*, SFN is metabolized to produce sulforaphane-glutathione (SFN-GSH), sulforaphanecysteine-glycine (SFN-CG), sulforaphane-cysteine (SFN-Cys), and sulforaphane-N-acetylcysteine (SFN-NAC) via mercapturic acid pathway (5,8,9). Further studies showed that SFN induced cell apoptosis, inhibited cell proliferation, invasion and angiogenesis (10-14). In human glioblastoma cells, it has been reported that SFN induced apoptosis (15) and our previous study showed that SFN inhibited cell invasion via ERK1/2 signaling pathway (12). Compared with SFN, SFN-Cys inhibits histone deacetylase (HDAC) more efficiently and has longer half-life and retention time *in vivo* (8,16). HDAC is highly related to cell growth. Hence we assume that SFN-Cys inhibits cell growth and induces apoptosis with higher efficiency, it is important to investigate the underlying mechanisms. These results will provide new insight into the SFN analog anticancer effect, so that we might develop new anticancer agents.

The extracellular signal-regulated kinases (ERK1/2) regulate many cellular responses by phosphorylating a number of downstream effectors (12,13,17-20). Transient phosphorylation of ERK1/2 (5-15-min stimulation) contributes to cell growth (18) while sustained phosphorylation of ERK1/2 (>15 min stimulation) causes cell apoptosis (19). Our previous studies demonstrated that SFN inhibited invasion by sustained activation of ERK1/2 to regulate E-cadherin and CD44v6 in human prostate cancer DU145 cells (13) and SFN-Cys suppressed invasion by sustained phosphorylation of ERK1/2 and downregulating galectin-1 in human prostate cancer DU145 and PC3 cells (20). Moreover, SFN inhibited invasion via activating ERK1/2 signaling in human glioblastoma U87MG and U373MG cells. Therefore, we hypothesized that

Correspondence to: Professor Wei Wu, Department of Biochemistry and Molecular Biology, School of Basic Medical Sciences, Capital Medical University, 10 Xitoutiao, You An Men Wai Ave., Feng Tai, Beijing 100069, P.R. China
E-mail: weiwu207@ccmu.edu.cn

Key words: sulforaphane-cysteine, ERK1/2, cleaved caspase 3, apoptosis, glioblastoma

SFN-Cys might induce apoptosis by activating ERK1/2 and the apoptosis-related proteins.

Both Bax and Bcl-2 are members of the Bcl-2 family regulating the apoptosis of glioblastoma cells (21). Bax contributes to the apoptotic response of glioblastoma cells and the overexpression of Bax increases survival of glioblastoma patients (22). Downregulation of Bcl-2 effectively induced apoptosis in glioblastoma cells (23), while overexpression of Bcl-2 inhibited apoptosis and decreased the effect of radiotherapy or chemotherapy in many other cancers (24). The apoptosis-inducing ability of Bax is suppressed by Bcl-2 binding to its homologous C-terminal domain (25-27). Thus, the increasing Bax/Bcl-2 ratio results in apoptosis in human glioblastoma cells while the decreasing Bax/Bcl-2 ratio represses cell apoptosis and contributes to the resistance of glioblastoma cells to chemotherapeutic agent (28). It is reported that the upregulation of Bax/Bcl-2 resulted in the loss of mitochondrial membrane potential (MMP), inducing cell apoptosis via the intrinsic pathway in glioma cells (29). Since the ratio of Bax/Bcl-2 is regulated by ERK1/2 signaling pathway (30), we hypothesized that SFN-Cys might induce intrinsic apoptosis by upregulating Bax/Bcl-2 ratio mediated via the activated ERK1/2.

Cysteine-aspartic proteases (caspases) constitute a family of proteolytic enzymes and are largely known for their functions in apoptosis (31). The caspases are divided into two groups, the initiator caspases such as caspase 8 and 9 and the effector caspases such as caspase 3 (32,33). Caspase 3 exists as an inactive proenzyme while it is activated after cleaved by initiator caspases (34). Cleaved caspase 3 in turn cleaves multiple cell substrates such as poly(ADP-ribose) polymerase (PARP), leading to cell apoptosis (35). It is reported that SFN activated caspase 3 via ERK1/2 pathway, leading to cell apoptosis in human glioblastoma cells (36). Additionally, caspase 3 is a downstream protein of Bax/Bcl-2, and the upregulation of Bax/Bcl-2 ratio leads to the activation of caspase 3 (28). Taken together, we thought that SFN-Cys might activate ERK1/2, increasing the ratio of Bax/Bcl-2 and upregulating cleaved caspase 3, which led to cell apoptosis in U373MG and U87MG cells. Altogether, our results provide evidence for SFN-Cys inducing apoptosis in glioblastoma, and further explore the underlying mechanisms, facilitating finding more natural products for treating glioblastoma.

Materials and methods

Reagents. D, L-Sulforaphane-L-cysteine (SFN-Cys) and caspase 3 antibody were from Santa Cruz Biotechnology (Santa Cruz, CA, USA). DMEM/HIGH glucose culture medium was from Hyclone (Logan, UT, USA). Fetal bovine serum (FBS) was from Zhejiang Tianhang Biological Technology Co., Ltd. (Zhejiang, China). Penicillin-streptomycin was from Invitrogen (Carlsbad, CA, USA). Dimethyl sulfoxide (DMSO) was acquired from AppliChem GmbH (Ottoweg4, D-64291 Darmstadt, Germany). β-actin antibody was from Proteintech Group, Inc. (Chicago, IL, USA). CCK8 assay kit was from Dojindo Laboratories (Shanghai, China). Annexin V-FITC Apoptosis assay kit was acquired from Genstar (Beijing, China). Mitochondrial membrane potential assay kit with JC-1 was from Beyotime Biotechnology (Shanghai, China). pERK1/2 antibody, ERK1/2 antibody and PD98059 were acquired from Cell Signaling Technology, Inc. (Shanghai, China). The antibodies against Bax and Bcl-2 were from Sangon Biotech (Shanghai, China).

Cell culture. Human glioblastoma U87MG cell line was purchased from the Cell Resource Center, Peking Union Medical College (CRC/PUMC) and U373MG cell line was purchased from American Type Culture Collection (ATCC, Manassas, VA, USA). Cells were cultured in DMEM/HIGH glucose culture medium supplemented with 10% FBS, 100 U/ml penicillin and 100 U/ml streptomycin in a standard humidified incubator with 5% CO_2 at 37˚C. The cells were treated with SFN-Cys for 24 h and pretreated with ERK1/2 inhibitor PD98059 (25 μM) for 30 min.

Morphological observation. U373MG and U87MG cells were seeded in 6-well culture plates and not exposed to SFN-Cys with different concentrations (0, 15, 30, and 45 μM) for 24 h until the cells were grown to 70% confluence. Cell morphology was observed with phase-contrast microscope at x100 magnification (Leica, Mannheim, Germany) and documented by the digital camera (Olympus, Tokyo, Japan) connected to the microscope.

Cell viability assay. The cell viability was evaluated by utilizing the Cell Counting Kit-8 (CCK-8) assay. Cells were seeded in 96-well plates at $5x10^3$ cells/well and treated with various doses of SFN-Cys for 24 h. Then 20 μl CCK-8 reagents were added to each well and the 96-well plate was incubated at 37˚C for an additional 30 min. Then the absorbance was measured at 450 nm by a BioTek microplate reader (Synergy™ HT, BioTek Instruments, Inc., Winooski, VT, USA).

Flow cytometry analysis of apoptosis. Apoptosis was assessed by utilizing Annexin V-FITC/propidium iodide (PI) staining followed by flow cytometry. The cells were plated in 6-well plates and incubated with various concentrations of SFN-Cys (0, 15, 30 and 45 μM). After incubated for 24 h, cells were collected and centrifuged at 1000 rpm for 5 min. Then cells were washed twice with cold PBS to remove excessive medium. Next, the cells were re-suspended at a concentration of $1x10^6$ cells/ml in binding buffer and incubated with annexin for 5 min V-FITC and PI was added afterwards at room temperature in the dark. All samples were analyzed on flow cytometry (FACSAria, BD Biosciences, San Jose, CA, USA) to determine the cell apoptotic rate.

Western blot analysis. Cells were collected and lysed with RIPA (Thermo Scientific, Waltham, MA, USA) combined with protease inhibitors (Roche, Mannheim, Germany) for 30 min. The cell lysate was centrifuged at 12,000 rpm for 15 min. Samples were separated on SDS-PAGE gels and then transferred to nitrocellulose membranes. Membranes were blocked with 1.5% BSA in TBS Tween-20 (TBS-T) buffer for 1 h and then incubated with primary antibody at 4˚C overnight. Afterwards, the membrane was washed with TBS-T for 30 min and then incubated with the fluorescence-labeled secondary antibody (LI-COR Bioscience, Lincoln, NE, USA)

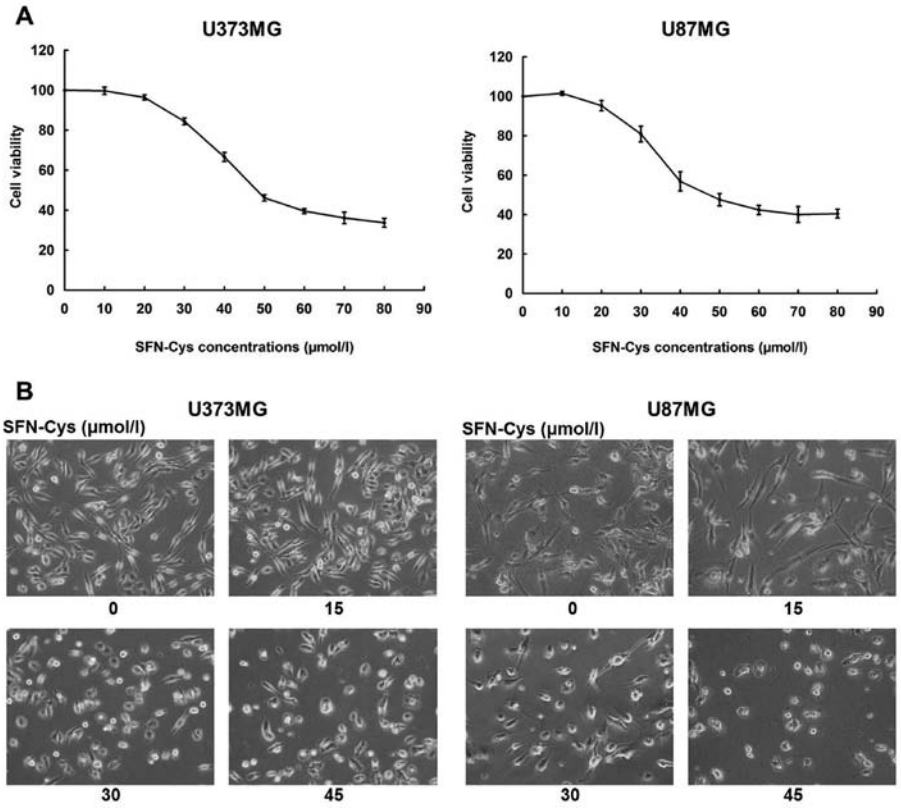

Figure 1. SFN-Cys inhibits cell viability and changes cell morphology in U373MG and U87MG cells. (A) U373MG and U87MG cells were incubated in the medium with increasing concentrations of SFN-Cys (0, 10, 20, 30, 40, 50, 60, 70 and 80 μM) for 24 h. Cell viability was determined by CCK-8 assay and shown as the percentage of control. Data are presented as the mean ± SD of three independent experiments. (B) U373MG and U87MG cells were treated with 0, 15, 30 and 45 μM SFN-Cys for 24 h. Cell morphology was observed by Leica DMIRB microscope at x100 magnification.

for 1 h. After washing, the membrane was scanned by Odyssey Infrared Imaging System (LI-COR Bioscience). The same membrane was stripped and incubated with β-actin antibody for equal loading and normalization.

Mitochondrial membrane potential assay. Mitochondrial membrane potential (MMP) was examined by using the mitochondrial membrane potential kit with JC-1. The cells were plated in 24-well plate and treated with drugs for 24 h. Then, cells were washed with PBS three times and incubated with 250 μl culture medium and 250 μl JC-1 working solution for 20 min in the dark at 37˚C. After that, the cells were washed three times (3 min each time) with ice cold JC-1 washing buffer. Images were captured by a fluorescence microscope at x200 magnification (Axio Imager A2, Zeiss, Jena, Germany). Fluorescent intensity was analyzed by Image-Pro Plus and the level of MMP was calculated as the JC-1 aggregate/monomer ratio.

Statistical analysis. Data are expressed as mean ± SD and the differences among the groups were analyzed by one-way ANOVA. $P<0.05$ was considered to be statistically significant.

Results

SFN-Cys dose-dependently decreases cell viability and changed cell morphology. CCK-8 assay was utilized to examine the reduction of cell viability after cells were incubated with SFN-Cys in U373MG and U87MG cells. The cells were exposed to 0, 10, 20, 30, 40, 50, 60, 70 and 80 μM SFN-Cys for 24 h. SFN-Cys was found to decrease cell viability in a dose-dependent manner (Fig. 1). Moreover, we found that SFN-Cys decreased cell viability remarkably when cells were exposed to 30 μM SFN-Cys for 24 h (Fig. 1A). Cells treated with SFN-Cys of 0, 15, 30 and 45 μM for 24 h were observed by the light microscope. The cells treated by SFN-Cys were shrunken and exhibited rounded shape compared with the untreated cells. Microscopic images in Fig. 1B showed that the cell morphology exposed to 30 μM SFN-Cys for 24 h began to change.

SFN-Cys dose-dependently induces cell apoptosis. Flow cytometry was utilized to prove whether the decrease of cell viability and the changes of morphology (Fig. 1) were caused by cell apoptosis. The cells were treated with 0, 15, 30 and 45 μM SFN-Cys for 24 h before flow cytometry analysis. The cell apoptosis rates are displayed in Fig. 2. We found that SFN-Cys induced cell apoptosis in a dose-dependent manner in both U373MG and U87MG cells. In addition, compared with the untreated control, a significant increase of apoptosis rate was shown in 30 μM SFN-Cys treated cells. Moreover, apoptosis rate in U87MG cells was higher than that in U373MG cells, suggesting the distinct sensitivity to SFN-Cys between U87MG and U373MG cells. Taken together, we chose 30 μM SFN-Cys as an optimal concentration for the following studies.

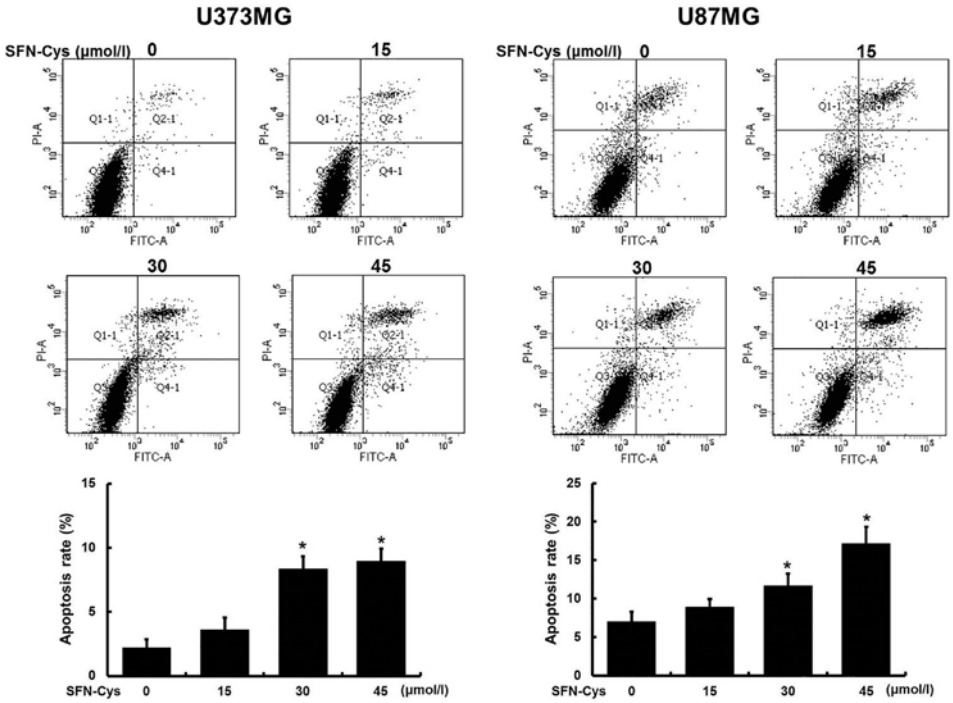

Figure 2. SFN-Cys dose-dependently induces cell apoptosis in U373MG and U87MG cells. U373MG and U87MG cells were treated with 0, 15, 30 and 45 μM SFN-Cys for 24 h. SFN-Cys induced an increase in both early apoptosis (Annexin V-positive, PI-negative) and late apoptosis (Annexin V/PI-double positive). Data are shown as means ± SD from three separate experiments. *P<0.05 vs. control group, n=3.

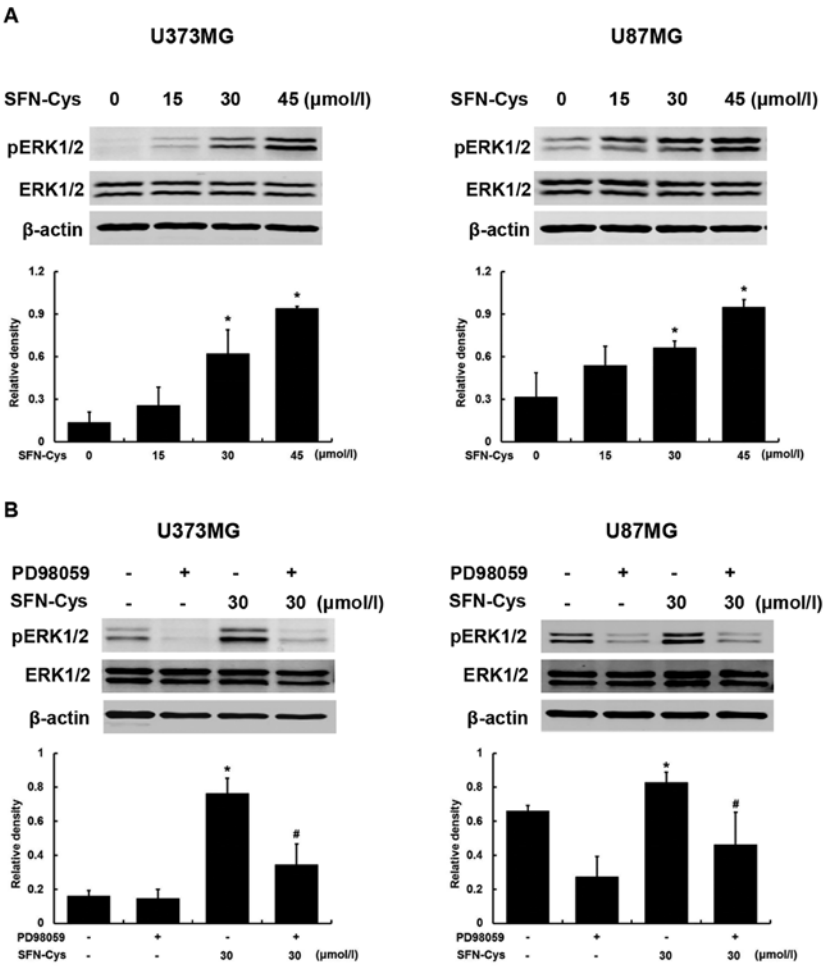

Figure 3. SFN-Cys dose-dependently induces ERK1/2 phosphorylation. U373MG and U87MG cells were treated with (A) varying concentrations of SFN-Cys (0, 15, 30 and 45 μM) for 24 h (B) 0 and 30 μM SFN-Cys respectively, PD98059 alone and SFN-Cys with PD98059 combination respectively for 24 h. Data are shown as means ± SD from three separate experiments. *P<0.05 vs. control group. #P<0.05 vs. SFN-Cys only group, n=3.

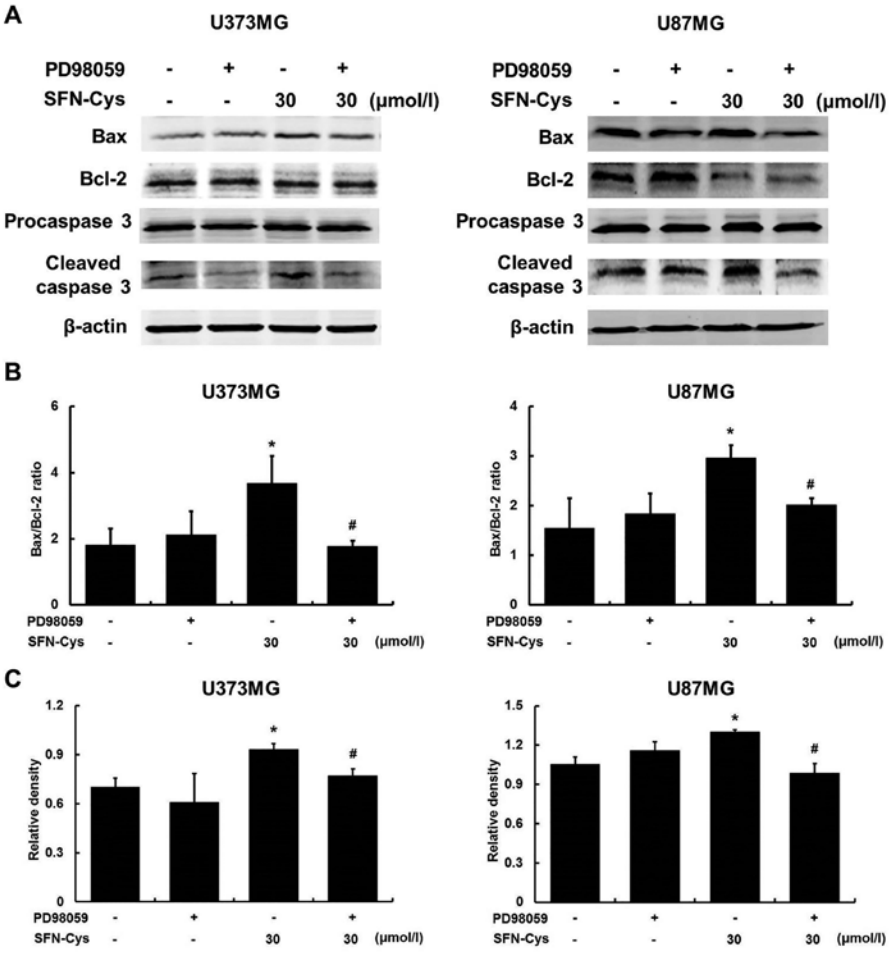

Figure 4. SFN-Cys increases the ratio of Bax/Bcl-2 and upregulates cleaved caspase 3 by activating ERK1/2. (A) U373MG and U87MG cells were treated with PD98059 only, SFN-Cys only and PD98059 plus SFN-Cys for 24 h. Western blot analysis was utilized to evaluate the levels of Bax, Bcl-2, procaspase 3 and cleaved caspase 3. (B) The ratio of Bax/Bcl-2 in (A). (C) The relative density of cleaved caspase 3 in (A). Data are shown as means ± SD from three separate experiments. *P<0.05 vs. control group. #P<0.05 vs. SFN-Cys only group, n=3.

SFN-Cys dose-dependently activates ERK1/2. U373MG and U87MG cells were treated with increasing doses of SFN-Cys (0, 15, 30 and 45 μM) for 24 h. Western blot analysis showed that SFN-Cys activated ERK1/2 (Thr202/Tyr204) in a dose-dependent way and pERK1/2 was significantly increased at 30 μM of SFN-Cys (Fig. 3A), which was in agreement with our previous studies that SFN and SFN-Cys contributed to the phosphorylation of ERK1/2 in prostate cancer cells (13,20). PD98059, ERK1/2 inhibitor, was utilized to investigate the role of ERK1/2 in SFN-Cys-induced apoptosis. Fig. 3B shows that the phosphorylation of ERK1/2 was significantly diminished in cells treated with both SFN-Cys (30 μM) and PD98059 (25 μM) compared with the cells treated with SFN-Cys alone.

SFN-Cys increases the ratio of Bax/Bcl-2 and upregulates cleaved caspase 3 by activating ERK1/2. Western blot analysis was utilized to evaluate the expression of the apoptosis regulatory proteins. We have already demonstrated that PD98059 blocked the ERK1/2 signaling pathway activated by SFN-Cys (Fig. 3B). As shown in Fig. 4, the ratio of Bax/Bcl-2 was increased in SFN-Cys-treated cells while the increased ratio was reversed by PD98059 in SFN-Cys with the PD98059 treated cells, indicating that Bax and Bcl-2 were the downstream effectors of ERK1/2. After cells were treated with SFN-Cys for 24 h, the expression of cleaved caspase 3 was significantly increased compared with the untreated cells. PD98059 reversed the expression of cleaved caspase 3 in both PD98059 and SFN-Cys treated cells compared with SFN-Cys only treated cells, suggesting that SFN-Cys induced cell apoptosis through sustained activation of ERK1/2 and subsequently activating caspase 3 in U373MG and U87MG cells. Altogether, these results indicated that SFN-Cys activated ERK1/2, increasing the ratio of Bax/Bcl-2 and upregulating cleaved caspase 3 in U373MG and U87MG cells.

SFN-Cys induces the loss of mitochondrial membrane potential (MMP) by activating ERK1/2. In order to confirm the intrinsic apoptosis pathway which was induced by SFN-Cys, JC-1 mitochondrial membrane potential assay was implemented to analyze mitochondrial membrane potential. Red fluorescence indicated JC-1 aggregated in cells with high MMP, while green fluorescence indicated that JC-1 was presented as a monomer in cells with depolarized mitochondria. In Fig. 5A, the green fluorescence was increased and the red fluorescence was decreased in SFN-Cys only treated cells compared with that in untreated cells. Compared with SFN-Cys only treated cells,

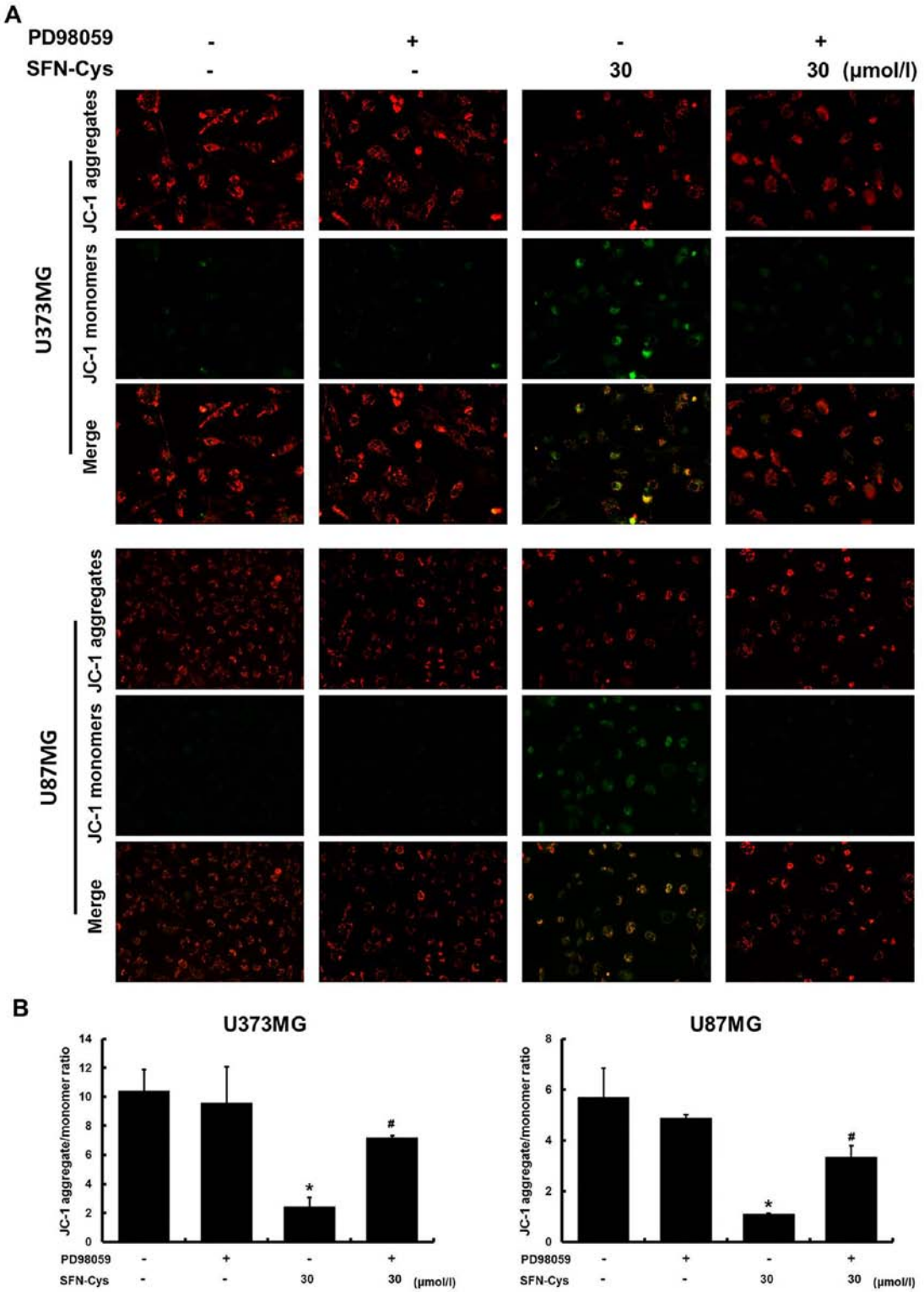

Figure 5. SFN-Cys induces the loss of mitochondrial membrane potential (MMP) by activating ERK1/2. (A) U373MG and U87MG cells were treated with PD98059 only, SFN-Cys only and PD98059 plus SFN-Cys for 24 h. The level of MMP was examined by the mitochondrial membrane potential assay kit with JC-1. Images were captured by a fluorescence microscope at x200 magnification (Zeiss Imager A2). (B) Quantification of the relative level of MMP in (A). Data are shown as means ± SD from three separate experiments. *P<0.05 vs. control group. #P<0.05 vs. SFN-Cys only group, n=3.

both PD98059 and SFN-Cys treated cells exhibited decreased green fluorescence and the restoration of the red fluorescence. As shown in Fig. 5B, the level of MMP in SFN-Cys only treated cells was significantly decreased compared with the untreated cells. PD98059 reversed the level of MMP in both SFN-Cys and PD98059 treated cells compared with SFN-Cys only treated cells, thus indicating that SFN-Cys induced the loss of MMP which could be reversed by PD98059. Taken together, SFN-Cys induced the loss of MMP by activating ERK1/2.

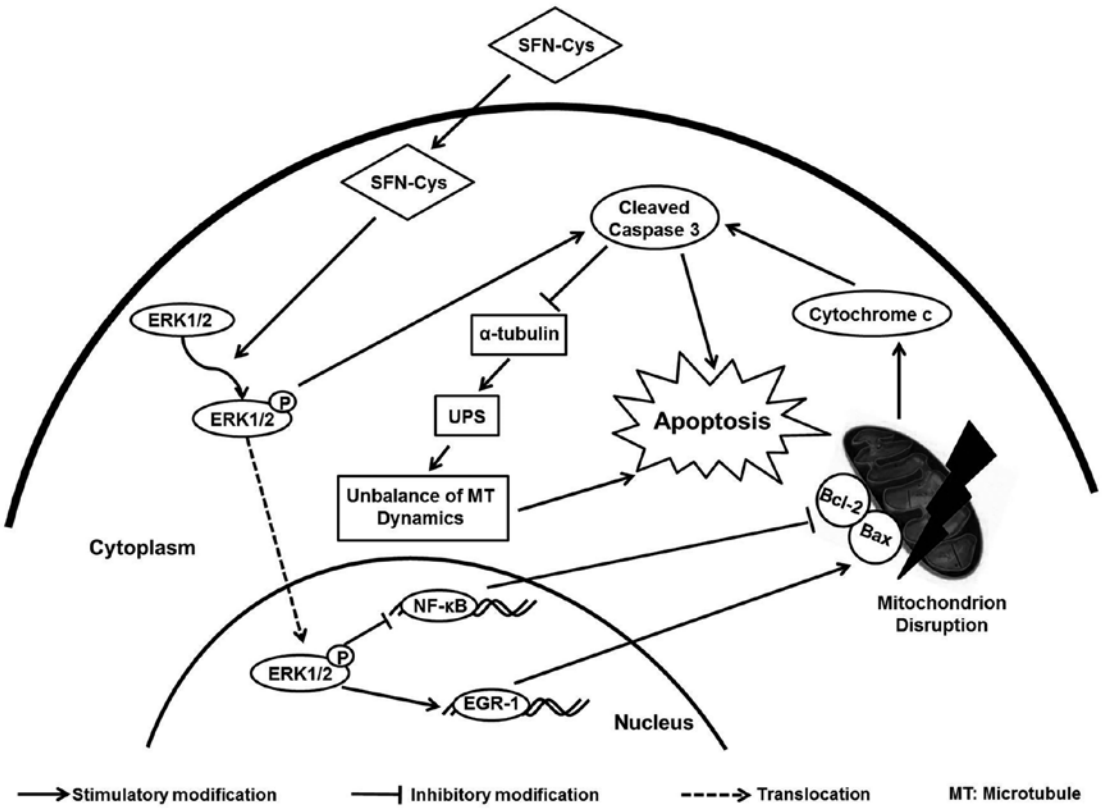

Figure 6. The proposed signaling map for SFN-Cys-induced apoptosis in human glioblastoma cells.

Discussion

Dietary bioactive components of natural products have been extensively studied for cancer prevention and treatment with low toxicity (37). Of all, sulforaphane (SFN) was demonstrated to be the safest for human cancer therapy (38). Here we demonstrated that sulforaphane-cysteine (SFN-Cys), as a metabolite of SFN *in vivo*, has potentiality to induce apoptosis. By treating mice with 20 μmoles SFN, SFN was undetectable in brain by 2 h, while SFN-Cys was abundantly detectable in brain by 6 h, indicating that SFN-Cys could penetrate the blood-brain barrier (BBB) to target the tumor with a longer half-life compared with SFN *in vivo* (8).

The specific hydroxamic acid group of SFN-Cys has greater affinity for Zn^{2+} of histone deacetylase (HDAC) while SFN has little effect, suggesting that SFN-Cys has the most potentiality to inhibit HDAC (16). Our previous results showed that SFN-Cys inhibited invasion in human prostate cancer cells (20), herein the underlying mechanisms by which SFN-Cys induced cell apoptosis in human glioblastoma cells is demonstrated.

Both SFN-Cys and SFN could significantly decrease cell viability and induce apoptosis at 30 μM as an optimal concentration in U373MG cells and U87MG cells. The IC_{50} of SFN-Cys was approximately 45 μM (Fig. 1A) while the IC_{50} of SFN was ~60 μM (12), suggesting that SFN-Cys was a more effective anticarcinogen than SFN. In previous studies, we demonstrated that ERK1/2 was sustainedly activated by SFN-Cys (20 μM) within 48 h in U373MG and U87MG cell lines (data not shown). Sustained activation of ERK1/2 mediated by SFN-Cys is a key trigger to induce apoptosis. The downstream effectors might be involved in apoptosis-related signaling pathways, such as the death receptor pathway and the mitochondria-related pathways. We further demonstrated that SFN-Cys (30 μM) induced cell apoptosis by upregulating Bax/Bcl-2 ratio and causing the loss of mitochondrial membrane potential (MMP) through activating ERK1/2. Apoptosis might also involve multiple transcription factors, including early growth response 1 (EGR-1) and nuclear factor-κB (NF-κB) (39-41). EGR-1 is known to be activated by ERK1/2 and it can bind to the Bax gene promoter to induce the expression of Bax (42,43). Given that SFN activates EGR-1 in glioblastoma (44), SFN-Cys might upregulate Bax by activating EGR-1 mediated by the ERK1/2 signaling pathway. NF-κB can be downregulated by ERK1/2 and the activation of NF-κB contributes to the upregulation of Bcl-2 (45,46). Besides, it was shown that SFN suppressed the activation of NF-κB to induce cell apoptosis, suggesting that SFN-Cys may downregulate Bcl-2 by suppressing the activation of NF-κB mediated by phosphorylating ERK1/2. We also demonstrated that SFN-Cys activated caspase 3 via the ERK1/2 signaling pathway, however, whether SFN-Cys activates caspase 3 by upregulating Bax/Bcl-2 ratio mediated by ERK1/2 is still unclear. The possible cause of the activation of caspase 3 is the release of cytochrome *c* from the mitochondria regulated by Bax/Bcl-2 (22,47). Bax, Bcl-2, caspase 3 and the disruption of MMP are the hallmarks of intrinsic apoptosis pathway, suggesting that SFN-Cys induced cell apoptosis in human glioblastoma cells via the intrinsic apoptosis pathway. Therefore, the underlying mechanism of caspase 3 activation is likely to be that the SFN-Cys-mediated

increase of Bax/Bcl-2 ratio acts as an apoptotic stimulus resulting in MMP disruption, triggering the release of cytochrome *c* into the cytosol which then activates caspase 9 and activates caspase 3 subsequently via the ERK1/2 signaling pathway. Alternatively, in addition to cytochrome *c*, second mitochondria-derived activator of caspases (Smac) can be released into the cytosol as well and bind to the inhibitor of apoptosis (IAP) proteins to deactivate them, resulting in caspase 3 activation and cell death eventually (48). It can be inferred that SFN-Cys may also induce cell apoptosis by triggering the release of Smac and subsequently deactivating the IAP proteins or just regulating the IAP proteins to deactivate them directly. Apart from the intrinsic apoptosis pathway, apoptosis is also sub-classified into two other types of death pathways; the death receptor-mediated (extrinsic) pathway and the endoplasmic-reticulum (ER) stress-mediated apoptosis pathway. The extrinsic pathway involves death receptors, from the tumor necrosis factor (TNF) superfamily, to transmit death signal from the surface to the intracellular signaling pathways, leading to the activation of caspase 8 and the subsequent activation of caspase 3 (49-51). Also, the ER stress apoptosis pathway is triggered by the disturb folding proteins in the ER, leading to the activation of caspase 3 eventually (52). Since these two pathways could both be activated through the ERK1/2 signaling pathway (52,53) and lead to the activation of caspase 3, we thought that SFN-Cys might induce cell apoptosis not only via the intrinsic pathway but via the extrinsic pathway and the ER stress-mediated pathway as well in human glioblastoma cells.

It is reported that caspase 3 executes cell apoptosis, to demonstrate which, Abdi *et al* administered z-VAD fmk (a pan-caspase inhibitor) and z-DEVD fmk (a selective caspase 3 inhibitor) to cells, respectively, and both of the inhibitors resulted in complete inhibition of apoptosis (54). It can be inferred that activated caspase 3 was the executioner to cell apoptosis. Studies also showed that caspase 3 could cleave poly (ADP-ribose) polymerase (PARP) to deprive its abilities of detecting and repairing DNA damage, leading to cell apoptosis ultimately (35,55). The above suggested that the activated caspase 3 which was induced by SFN-Cys could cleave the specific substrates as a proteolytic enzyme, executing cell apoptosis. Thus, caspase 3 might cleave some other substrates in cancer cells as well, such as microtubule associated proteins which play a crucial role in cell apoptosis. In separate studies, we found that caspase 3 cleaved α-tubulin resulting in cell apoptosis (data not shown). The proteolytic activity of caspase 3 is also closely related to the ubiquitin-proteasome system (UPS): caspase 3 cleavage produces substrates such as actomyosin resulting in an increase of proteasome-mediated proteolysis (56). Given that SFN-Cys-activated caspase 3 might cleave α-tubulin to increase proteolysis of UPS, this excessive proteolysis will result in microtubule depolymerization and apoptosis (57). Taxol was used as a microtubule-stabilizing agent to prevent cancers, however, the glioblastoma cells often resist it (58). Luckily, it is reported that SFN could induce cell apoptosis in Taxol-resistant cells (59). These studies suggested that SFN-Cys might be a much more efficient microtubule-targeting agent compared with the traditional agent such as Taxol due to its versatile anticarcinogenic abilities. In addition, SFN can modulate epigenetic events. Previous studies showed that SFN induced cell apoptosis by regulating the level of epigenetic regulators such as polycomb group (PcG) proteins which contribute to chromatin structure modification and gene expression suppression. The SFN-mediated reduction of PcG proteins in a proteasome-dependent way led to an increase of cleaved caspase 3 and cell apoptosis (60). This was consistent with our hypothesis that SFN-Cys-mediated proteolysis of UPS led to cell apoptosis. Thus, we inferred that SFN-Cys might also activate caspase 3 and induce cell apoptosis by modulating the epigenetic regulators mediated via UPS. Moreover, HDAC inhibitor increased the level of caspase 3 mRNA (61). This evidence suggested that the expression of caspase 3 could be epigenetically regulated by HDAC. Recently, HDAC inhibitors are used in epigenetic glioblastoma therapies (62). Given that SFN-Cys was the most potential HDAC inhibitor among SFN and its metabolites, we think that SFN-Cys might induce cell apoptosis through the epigenetic regulation of caspase 3. Therefore, there are multiple ways for SFN-Cys to suppress the tumor progression and further studies needed to be done.

In conclusion, SFN-Cys upregulated Bax/Bcl-2 ratio and activated caspase 3 subsequently via sustained activating ERK1/2 signaling, leading to intrinsic apoptosis in human glioblastoma U373MG and U87MG cells (Fig. 6). The underlying mechanisms that SFN-Cys triggered provided us with more thoughts and information to develop new drugs to treat glioblastoma with high efficacy.

Acknowledgements

This study was supported by the National Natural Science Foundation of China (grant nos. 81272843 and 81601993).

References

1. Louis DN, Ohgaki H, Wiestler OD, Cavenee WK, Burger PC, Jouvet A, Scheithauer BW and Kleihues P: The 2007 WHO classification of tumours of the central nervous system. Acta Neuropathol 114: 97-109, 2007.
2. Gielen PR, Aftab Q, Ma N, Chen VC, Hong X, Lozinsky S, Naus CC and Sin WC: Connexin43 confers Temozolomide resistance in human glioma cells by modulating the mitochondrial apoptosis pathway. Neuropharmacology 75: 539-548, 2013.
3. Alifieris C and Trafalis DT: Glioblastoma multiforme: Pathogenesis and treatment. Pharmacol Ther 152: 63-82, 2015.
4. Abdull Razis AF and Noor NM: Cruciferous vegetables: Dietary phytochemicals for cancer prevention. Asian Pac J Cancer Prev 14: 1565-1570, 2013.
5. Clarke JD, Hsu A, Yu Z, Dashwood RH and Ho E: Differential effects of sulforaphane on histone deacetylases, cell cycle arrest and apoptosis in normal prostate cells versus hyperplastic and cancerous prostate cells. Mol Nutr Food Res 55: 999-1009, 2011.
6. Pham NA, Jacobberger JW, Schimmer AD, Cao P, Gronda M and Hedley DW: The dietary isothiocyanate sulforaphane targets pathways of apoptosis, cell cycle arrest, and oxidative stress in human pancreatic cancer cells and inhibits tumor growth in severe combined immunodeficient mice. Mol Cancer Ther 3: 1239-1248, 2004.
7. Karmakar S, Weinberg MS, Banik NL, Patel SJ and Ray SK: Activation of multiple molecular mechanisms for apoptosis in human malignant glioblastoma T98G and U87MG cells treated with sulforaphane. Neuroscience 141: 1265-1280, 2006.
8. Clarke JD, Hsu A, Williams DE, Dashwood RH, Stevens JF, Yamamoto M and Ho E: Metabolism and tissue distribution of sulforaphane in Nrf2 knockout and wild-type mice. Pharm Res 28: 3171-3179, 2011.
9. Dinkova-Kostova AT and Kostov RV: Glucosinolates and isothiocyanates in health and disease. Trends Mol Med 18: 337-347, 2012.

10. Yao A, Shen Y, Wang A, Chen S, Zhang H, Chen F, Chen Z, Wei H, Zou Z, Shan Y, *et al*: Sulforaphane induces apoptosis in adipocytes via Akt/p70s6k1/Bad inhibition and ERK activation. Biochem Biophys Res Commun 465: 696-701, 2015.
11. Wang L, Tian Z, Yang Q, Li H, Guan H, Shi B, Hou P and Ji M: Sulforaphane inhibits thyroid cancer cell growth and invasiveness through the reactive oxygen species-dependent pathway. Oncotarget 6: 25917-25931, 2015.
12. Li C, Zhou Y, Peng X, Du L, Tian H, Yang G, Niu J and Wu W: Sulforaphane inhibits invasion via activating ERK1/2 signaling in human glioblastoma U87MG and U373MG cells. PLoS One 9: e90520, 2014.
13. Peng X, Zhou Y, Tian H, Yang G, Li C, Geng Y, Wu S and Wu W: Sulforaphane inhibits invasion by phosphorylating ERK1/2 to regulate E-cadherin and CD44v6 in human prostate cancer DU145 cells. Oncol Rep 34: 1565-1572, 2015.
14. Shankar S, Ganapathy S and Srivastava RK: Sulforaphane enhances the therapeutic potential of TRAIL in prostate cancer orthotopic model through regulation of apoptosis, metastasis, and angiogenesis. Clin Cancer Res 14: 6855-6866, 2008.
15. Zhang Z, Li C, Shang L, Zhang Y, Zou R, Zhan Y and Bi B: Sulforaphane induces apoptosis and inhibits invasion in U251MG glioblastoma cells. Springerplus 5: 235, 2016.
16. Myzak MC, Karplus PA, Chung FL and Dashwood RH: A novel mechanism of chemoprotection by sulforaphane: Inhibition of histone deacetylase. Cancer Res 64: 5767-5774, 2004.
17. Deschênes-Simard X, Kottakis F, Meloche S and Ferbeyre G: ERKs in cancer: Friends or foes? Cancer Res 74: 412-419, 2014.
18. Tong WG, Ding XZ, Talamonti MS, Bell RH and Adrian TE: LTB4 stimulates growth of human pancreatic cancer cells via MAPK and PI-3 kinase pathways. Biochem Biophys Res Commun 335: 949-956, 2005.
19. Lee WJ, Hsiao M, Chang JL, Yang SF, Tseng TH, Cheng CW, Chow JM, Lin KH, Lin YW, Liu CC, *et al*: Quercetin induces mitochondrial-derived apoptosis via reactive oxygen species-mediated ERK activation in HL-60 leukemia cells and xenograft. Arch Toxicol 89: 1103-1117, 2015.
20. Tian H, Zhou Y, Yang G, Geng Y, Wu S, Hu Y, Lin K and Wu W: Sulforaphane-cysteine suppresses invasion via downregulation of galectin-1 in human prostate cancer DU145 and PC3 cells. Oncol Rep 36: 1361-1368, 2016.
21. Manero F, Gautier F, Gallenne T, Cauquil N, Grée D, Cartron PF, Geneste O, Grée R, Vallette FM and Juin P: The small organic compound HA14-1 prevents Bcl-2 interaction with Bax to sensitize malignant glioma cells to induction of cell death. Cancer Res 66: 2757-2764, 2006.
22. Cartron PF, Oliver L, Martin S, Moreau C, LeCabellec MT, Jezequel P, Meflah K and Vallette FM: The expression of a new variant of the pro-apoptotic molecule Bax, Baxpsi, is correlated with an increased survival of glioblastoma multiforme patients. Hum Mol Genet 11: 675-687, 2002.
23. George J, Banik NL and Ray SK: Combination of taxol and Bcl-2 siRNA induces apoptosis in human glioblastoma cells and inhibits invasion, angiogenesis and tumour growth. J Cell Mol Med 13: 4205-4218, 2009.
24. Wick W, Grimmel C, Wild-Bode C, Platten M, Arpin M and Weller M: Ezrin-dependent promotion of glioma cell clonogenicity, motility, and invasion mediated by BCL-2 and transforming growth factor-beta2. J Neurosci 21: 3360-3368, 2001.
25. Thomas S, Quinn BA, Das SK, Dash R, Emdad L, Dasgupta S, Wang XY, Dent P, Reed JC, Pellecchia M, *et al*: Targeting the Bcl-2 family for cancer therapy. Expert Opin Ther Targets 17: 61-75, 2013.
26. van Delft MF and Huang DC: How the Bcl-2 family of proteins interact to regulate apoptosis. Cell Res 16: 203-213, 2006.
27. Yin XM, Oltvai ZN and Korsmeyer SJ: BH1 and BH2 domains of Bcl-2 are required for inhibition of apoptosis and heterodimerization with Bax. Nature 369: 321-323, 1994.
28. Shi L, Chen J, Yang J, Pan T, Zhang S and Wang Z: MiR-21 protected human glioblastoma U87MG cells from chemotherapeutic drug temozolomide induced apoptosis by decreasing Bax/Bcl-2 ratio and caspase-3 activity. Brain Res 1352: 255-264, 2010.
29. Skała E, Sitarek P, Toma M, Szemraj J, Radek M, Nieborowska-Skorska M, Skorski T, Wysokińska H and Śliwiński T: Inhibition of human glioma cell proliferation by altered Bax/Bcl-2-p53 expression and apoptosis induction by *Rhaponticum carthamoides* extracts from transformed and normal roots. J Pharm Pharmacol 68: 1454-1464, 2016.
30. Yating Q, Yuan Y, Wei Z, Qing G, Xingwei W, Qiu Q and Lili Y: Oxidized LDL induces apoptosis of human retinal pigment epithelium through activation of ERK-Bax/Bcl-2 signaling pathways. Curr Eye Res 40: 415-422, 2015.
31. Nuñez G, Benedict MA, Hu Y and Inohara N: Caspases: The proteases of the apoptotic pathway. Oncogene 17: 3237-3245, 1998.
32. Riedl SJ and Shi Y: Molecular mechanisms of caspase regulation during apoptosis. Nat Rev Mol Cell Biol 5: 897-907, 2004.
33. Tait SW and Green DR: Mitochondria and cell death: Outer membrane permeabilization and beyond. Nat Rev Mol Cell Biol 11: 621-632, 2010.
34. Walters J, Pop C, Scott FL, Drag M, Swartz P, Mattos C, Salvesen GS and Clark AC: A constitutively active and uninhibitable caspase-3 zymogen efficiently induces apoptosis. Biochem J 424: 335-345, 2009.
35. Yu SW, Wang H, Poitras MF, Coombs C, Bowers WJ, Federoff HJ, Poirier GG, Dawson TM and Dawson VL: Mediation of poly(ADP-ribose) polymerase-1-dependent cell death by apoptosis-inducing factor. Science 297: 259-263, 2002.
36. Huang TY, Chang WC, Wang MY, Yang YR and Hsu YC: Effect of sulforaphane on growth inhibition in human brain malignant glioma GBM 8401 cells by means of mitochondrial- and MEK/ERK-mediated apoptosis pathway. Cell Biochem Biophys 63: 247-259, 2012.
37. Jiang H, Shang X, Wu H, Huang G, Wang Y, Al-Holou S, Gautam SC and Chopp M: Combination treatment with resveratrol and sulforaphane induces apoptosis in human U251 glioma cells. Neurochem Res 35: 152-161, 2010.
38. Shapiro TA, Fahey JW, Dinkova-Kostova AT, Holtzclaw WD, Stephenson KK, Wade KL, Ye L and Talalay P: Safety, tolerance, and metabolism of broccoli sprout glucosinolates and isothiocyanates: A clinical phase I study. Nutr Cancer 55: 53-62, 2006.
39. Alejandro EU and Johnson JD: Inhibition of Raf-1 alters multiple downstream pathways to induce pancreatic beta-cell apoptosis. J Biol Chem 283: 2407-2417, 2008.
40. Yuan S, Wen J, Cheng J,, Shen W, Zhou S, Yan W, Shen L, Luo A and Wang S: Age-associated up-regulation of EGR1 promotes granulosa cell apoptosis during follicle atresia in mice through the NF-κB pathway. Cell Cycle 15: 2895-2905, 2016.
41. Zhou Z, Lu X, Wang J, Xiao J, Liu J and Xing F: microRNA let-7c is essential for the anisomycin-elicited apoptosis in Jurkat T cells by linking JNK1/2 to AP-1/STAT1/STAT3 signaling. Sci Rep 6: 24434, 2016.
42. Al-Sarraj A and Thiel G: Substance P induced biosynthesis of the zinc finger transcription factor Egr-1 in human glioma cells requires activation of the epidermal growth factor receptor and of extracellular signal-regulated protein kinase. Neurosci Lett 332: 111-114, 2002.
43. Li L, Zhao LM, Dai SL, Cui WX, Lv HL, Chen L and Shan BE: Periplocin extracted from *cortex periplocae* induced apoptosis of gastric cancer cells via the ERK1/2-EGR1 pathway. Cell Physiol Biochem 38: 1939-1951, 2016.
44. Yang M, Teng W, Qu Y, Wang H and Yuan Q: Sulforaphene inhibits triple negative breast cancer through activating tumor suppressor Egr1. Breast Cancer Res Treat 158: 277-286, 2016.
45. Zhang DX, Ma DY, Yao ZQ, Fu CY, Shi YX, Wang QL and Tang QQ: ERK1/2/p53 and NF-κB dependent-PUMA activation involves in doxorubicin-induced cardiomyocyte apoptosis. Eur Rev Med Pharmacol Sci 20: 2435-2442, 2016.
46. Wang Q, Liu S, Tang Y, Liu Q and Yao Y: MPT64 protein from Mycobacterium tuberculosis inhibits apoptosis of macrophages through NF-κB-miRNA21-Bcl-2 pathway. PLoS One 9: e100949, 2014.
47. Sitarek P, Skała E, Toma M, Wielanek M, Szemraj J, Nieborowska-Skorska M, Kolasa M, Skorski T, Wysokińska H and Śliwiński T: A preliminary study of apoptosis induction in glioma cells via alteration of the Bax/Bcl-2-p53 axis by transformed and non-transformed root extracts of *Leonurus sibiricus* L. Tumour Biol 37: 8753-8764, 2016.
48. Fulda S and Vucic D: Targeting IAP proteins for therapeutic intervention in cancer. Nat Rev Drug Discov 11: 109-124, 2012.
49. Ashkenazi A and Dixit VM: Death receptors: Signaling and modulation. Science 281: 1305-1308, 1998.
50. Hengartner MO: The biochemistry of apoptosis. Nature 407: 770-776, 2000.
51. Indran IR, Tufo G, Pervaiz S and Brenner C: Recent advances in apoptosis, mitochondria and drug resistance in cancer cells. Biochim Biophys Acta 1807: 735-745, 2011.
52. Sano R and Reed JC: ER stress-induced cell death mechanisms. Biochim Biophys Acta 1833: 3460-3470, 2013.

53. Cagnol S and Chambard JC: ERK and cell death: Mechanisms of ERK-induced cell death - apoptosis, autophagy and senescence. FEBS J 277: 2-21, 2010.
54. Abdi A, Sadraie H, Dargahi L, Khalaj L and Ahmadiani A: Apoptosis inhibition can be threatening in Aβ-induced neuroinflammation, through promoting cell proliferation. Neurochem Res 36: 39-48, 2011.
55. Virág L and Szabó C: The therapeutic potential of poly(ADP-ribose) polymerase inhibitors. Pharmacol Rev 54: 375-429, 2002.
56. Wang XH and Mitch WE: Muscle wasting from kidney failure - a model for catabolic conditions. Int J Biochem Cell Biol 45: 2230-2238, 2013.
57. Sung M and Giannakakou P: BRCA1 regulates microtubule dynamics and taxane-induced apoptotic cell signaling. Oncogene 33: 1418-1428, 2014.
58. Giussani P, Bassi R, Anelli V, Brioschi L, De Zen F, Riccitelli E, Caroli M, Campanella R, Gaini SM, Viani P, *et al*: Glucosylceramide synthase protects glioblastoma cells against autophagic and apoptotic death induced by temozolomide and Paclitaxel. Cancer Invest 30: 27-37, 2012.
59. Chen H, Landen CN, Li Y, Alvarez RD and Tollefsbol TO: Epigallocatechin gallate and sulforaphane combination treatment induce apoptosis in paclitaxel-resistant ovarian cancer cells through hTERT and Bcl-2 down-regulation. Exp Cell Res 319: 697-706, 2013.
60. Balasubramanian S, Chew YC and Eckert RL: Sulforaphane suppresses polycomb group protein level via a proteasome-dependent mechanism in skin cancer cells. Mol Pharmacol 80: 870-878, 2011.
61. Yakovlev A, Khafizova M, Abdullaev Z, Loukinov D and Kondratyev A: Epigenetic regulation of caspase-3 gene expression in rat brain development. Gene 450: 103-108, 2010.
62. Lee P, Murphy B, Miller R, Menon V, Banik NL, Giglio P, Lindhorst SM, Varma AK, Vandergrift WA III, Patel SJ, *et al*: Mechanisms and clinical significance of histone deacetylase inhibitors: Epigenetic glioblastoma therapy. Anticancer Res 35: 615-625, 2015.